Synthesis and self-assembly of temperature-responsive copolymers based on N-vinylpyrrolidone and triethylene glycol methacrylate

Journal:	*Polymer Chemistry*
Manuscript ID:	PY-ART-03-2015-000483.R1
Article Type:	Paper
Date Submitted by the Author:	22-Apr-2015
Complete List of Authors:	Jumeaux, Coline; Imperial College London, Department of Materials Chapman, Robert; Imperial College London, Department of Materials Chandrawati, Rona; Imperial College London, Department of Materials Stevens, Molly; Imperial College London, Department of Materials

Polymer Chemistry

RSCPublishing

ARTICLE

Synthesis and self-assembly of temperature-responsive copolymers based on *N*-vinylpyrrolidone and triethylene glycol methacrylate

Cite this: DOI: 10.1039/xoxxoooooox

Received ooth January 2012,
Accepted ooth January 2012

DOI: 10.1039/xoxxoooooox

www.rsc.org/

Coline Jumeaux, Robert Chapman, Rona Chandrawati, and Molly M. Stevens*

Polyvinylpyrrolidone (PVP) is a biocompatible, water-soluble polymer with unique physicochemical properties and attractive biological features that has found widespread use in several industries. Owing to advances in controlled polymerisation techniques, PVP can be easily synthesised with robust control over its architecture. However, the synthesis of PVP copolymers, which can allow tailoring of its properties and expand the scope of this polymeric material, is challenging and rarely reported. Here, we demonstrate the synthesis of well-defined, temperature-responsive polyvinylpyrrolidone-*co*-poly(triethylene glycol methacrylate) (PVP-*co*-pTEGMA) block copolymers *via* successive Reversible Addition-Fragmentation chain Transfer (RAFT) and Activators ReGenerated by Electron Transfer Atom Transfer Radical Polymerisation (ARGET-ATRP) techniques. We show that PVP-*co*-pTEGMA block copolymers display temperature-responsive behaviour and self-assemble above their cloud point temperature (T_{cp}) to form spherical nanostructures of 100-200 nm in diameter. Finally, we demonstrate stabilisation of these assemblies below their T_{cp} by cross-linking through the PVP block.

Introduction

Polyvinylpyrrolidone (PVP) is a non-toxic, non-ionic, water-soluble polymer with unique physicochemical properties. PVP has been widely used in many applications including food, cosmetics, and biomedicine. Its biocompatibility and anti-fouling properties are particularly attractive and have resulted in the application of PVP in the development of biomaterials and drug delivery carriers.[1–4] PVP has the ability to adhere to a number of substrates and can serve as a protective agent against aggregation of colloids. It can also act as a reducing agent for the formation of metallic nanoparticles from metal salts, and for this reason PVP has also been extensively used in biosensing[5] and the preparation of nanomaterials.[6–8]

The properties of PVP can be varied to meet the needs of specific applications by finely tuning the molecular weight of the polymer. This requires controlled polymerisation using techniques such as Reversible Addition-Fragmentation chain Transfer (RAFT) and Atom Transfer Radical Polymerisation (ATRP).[9–11] While the synthesis of PVP *via* ATRP has only rarely been reported,[12] several groups successfully synthesised PVP *via* RAFT.[13,14] In RAFT polymerisation, the choice of the chain transfer agent (CTA) is based on the monomers and is crucial for obtaining a suitable equilibrium between dormant and active species and robust control over the molecular weight of the polymer. The monomer, *N*-vinylpyrrolidone (NVP), has a low activity: it is non-conjugated and its radicals are poorly stable. Therefore, the Z group of the CTA must also be poorly stabilised in order to enable fast fragmentation of the polymer growing chains. This is typically done using a xanthate or dithiocarbamate (CTA) due to their reduced reactivity, allowing both radical addition and fragmentation.[15,16] PVP properties can also be altered by copolymerisation with another monomer, which will significantly expand the scope of this polymeric material. Statistical copolymers containing NVP and other monomers can in theory be synthesised in a single polymerisation, however this design can compromise the unique physicochemical properties of each monomer. Block copolymer structures are therefore more attractive because each component retains its individual properties. However, the preparation of block copolymers with PVP is challenging since all available RAFT agents for controlling its polymerisation are not suitable for the polymerisation of more active conjugated monomers such as styrene, acrylate and methacrylate.[9,17]

Due to these difficulties, the use of PVP block copolymers is virtually unexplored. As a result of the hydrogen bonding and biological properties of PVP, we expect that block copolymers of PVP and stimuli-responsive polymers will be very attractive for the preparation of complex architectures and nanomaterials for controlled drug release applications. Several strategies exist to prepare block copolymers of monomers with divergent

activity.[18] The first approach is to use click chemistry to link together two independently-prepared homopolymers.[19] However, the synthetic complexity involved makes this process unattractive for high molecular weight copolymers where complete reaction conversions are difficult to achieve. An alternative approach is to use 'switchable', stimuli-responsive dithiocarbamate RAFT agents, where protonation/deprotonation of the amide results in modulation of the strength of the Z-C=S bond, and in turn of its reactivity towards different monomers. This enables the synthesis of block copolymers with monomers of disparate reactivities by introduction of a Lewis acid between the two polymerisations.[20,21] To our knowledge, this technique has yet to be applied to the preparation of a wide range of copolymers. A third strategy involves the independent use of two different polymerisation mechanisms for each block extension.[22] This approach has been exploited to prepare PVP-*co*-poly(ε-caprolactone) block copolymers using either RAFT,[23] or ATRP,[24] to polymerise the NVP and ring opening polymerisation for the caprolactone. Matyjaszewski and coworkers recently used a dual RAFT / ATRP chloroxanthate CTA to prepare block copolymers of NVP with styrene (St), methyl acrylate (MA), and methyl methacrylate (MMA).[25] In this example the CTA was able to control the NVP polymerisation by RAFT, and then initiate chain extension with the more active monomer by ATRP, enabling the versatility of free radical polymerisation to be exploited in both blocks.[26]

We decided to use a similar approach to explore the synthesis of a range of novel temperature-responsive PVP block copolymers by copolymerising NVP with triethylene glycol methacrylate (TEGMA). pTEGMA is a non-linear PEG analogue and is stimuli-responsive, displaying a Lower Critical Solution Temperature (LCST) in aqueous media.[27,28] The synthesis of temperature-responsive anti-fouling polymers is not only of great interest for the design of temperature-responsive drug delivery carriers but also for surface modification for the development of cell sheet engineering in regenerative medicine.[29]

In this paper, we: (i) synthesise well-defined PVP-*co*-pTEGMA block copolymers by successive RAFT and Activators ReGenerated by Electron Transfer (ARGET)-ATRP; (ii) explore the temperature-responsive properties of these polymers; (iii) investigate the self-assembly properties of the PVP-*co*-pTEGMA block copolymers; and (iv) exploit cross-linking strategy to stabilise the self-assembled structure below the LCST. Synthesis of the block copolymers is performed using a dual RAFT and ATRP CTA. We use the RAFT moiety to polymerise NVP and the ATRP initiator to perform chain extensions with TEGMA *via* ARGET-ATRP.[30] Given the extensive interest in both temperature-responsive polymers and PVP, we anticipate these polymers will find rapid application in preparation of responsive materials for drug delivery or biomedical applications.

Experimental

Materials

Acetone, ascorbic acid, azobisisobutyronitrile (AIBN), 2,2'-bipyridine, α-bromoisobutyryl bromide, copper(II) chloride ($CuCl_2$), ethylene glycol, 1,4-dioxane, methacryloyl chloride, potassium ethyl xanthogenate, potassium persulphate, tetrahydrofuran (THF), triethylamine, triethylene glycol monomethyl ether, tris(pyridin-2-ylmethyl)amine (TPMA), 1,3,5-trioxane, *N*-vinylpyrrolidone (NVP) were purchased from Sigma Aldrich (UK) and were used without further purification. Dichloromethane (DCM) was purchased from AGTC Bioproducts (UK). Ethyl acetate and hexane were purchased from VWR Chemicals (UK). Copper(I) chloride (CuCl) was purchased from Sigma Aldrich (UK) and purified prior to use by stirring the powder in glacial acetic acid for 2 h. The white solids were filtered, washed thoroughly with cold ethanol, dried *in vacuo*, and stored under nitrogen.

Synthesis of triethylene glycol methacrylate (TEGMA)

Triethylene glycol monomethyl ether (5.0 g, 30 mmol) was added in a 50 mL two-necked round-bottom flask at 0 °C. The flask was equipped with a magnetic stirrer and an isobar addition funnel, and flushed with nitrogen (N_2). Dry DCM (20 mL) was added, followed by triethylamine (5.5 mL, 40 mmol), and dropwise addition of methacryloyl chloride (6.3 g, 60 mmol) in DCM (10 mL). After addition, the funnel was further rinsed with 5 mL of DCM and the mixture was stirred for 1 h at 0 °C and 17 h at room temperature. After addition of methanol to quench the reaction, the mixture was filtered to remove the triethylammonium chloride salt. The organic phase was washed with aqueous HCl (pH 2, 2 x 50 mL), aqueous NaOH (pH 12, 2 x 50 mL) and brine (2 x 50 mL), and dried over magnesium sulphate ($MgSO_4$) to yield the product as a yellow viscous oil (7.7 g, quantitative). ^{1}H NMR (400 MHz, $CDCl_3$, δ, ppm): 6.13-6.10 (m, 1H, =C<u>H</u>H), 5.58-5.54 (m, 1H, =CH<u>H</u>), 4.30-4.28 (m, 2H, COOC<u>H</u>$_2$CH$_2$O), 3.75-3.72 (m, 2H, COOCH$_2$C<u>H</u>$_2$O), 3.67-3.62 (m, 6H, OC<u>H</u>$_2$C<u>H</u>$_2$OC<u>H</u>$_2$), 3.55-3.52 (m, 2H, C<u>H</u>$_2$OCH$_3$), 3.37 (s, 3H, OC<u>H</u>$_3$), 1.93 (s, 3H, C<u>H</u>$_3$).

Synthesis of chloroxanthate CTA

2-hydroxyethyl 2-bromo-2-methylpropanoate (**1**): Ethylene glycol (31.03 g, 0.5 mol) and pyridine (0.72 g, 0.01 mol) were introduced to a 100 mL round bottom flask with dry THF (10 mL). The reaction mixture was cooled in an ice-water bath, and a solution of α-bromoisobutyryl bromide (1.07 mL, 0.01 mol) in dry THF (5 mL) was slowly added while stirring. The reaction mixture was stirred at 0 °C for 1 h and then at room temperature for 16 h. The reaction mixture was then diluted in aqueous HCl (pH 2) and extracted with DCM. The organic fractions were combined, extracted with water, washed with brine, dried on $MgSO_4$, filtered and evaporated to dryness to afford the product **1** as a colourless oil (1.83 g, 87 %). ^{1}H NMR

(400 MHz, $CDCl_3$, δ, ppm): 4.35-4.30 (m, 2H, C$\underline{H}_2$CH$_2$OH), 3.92-3.85 (m, 2H, C$\underline{H}_2$OH), 1.96 (s, 6H, (C$\underline{H}_3$)$_2$).

S-2-((2-hydroxyethoxy)carbonyl)propan-2-yl O-ethyl carbondithioate (**2**): Potassium ethyl xanthogenate (726 mg, 4.5 mmol) and acetone (10 mL) were added to a 50 mL round bottom flask equipped with a magnetic stirrer and a dropping funnel. A solution of 2-hydroxyethyl 2-bromo-2-methylpropanoate **1** (853 mg, 4.0 mmol) in acetone (10 mL) was added dropwise over 30 min and the reaction mixture was stirred for 17 h at room temperature. After filtration to eliminate the salts, the mixture was concentrated *in vacuo* to afford a yellow viscous solid. This was diluted using DCM (100 mL), washed with water (2 x 50 mL), dried over $MgSO_4$ and evaporated to dryness. The yellow viscous solid obtained was purified over a silica column (hexane : ethyl acetate 1:1), and the relevant fractions were combined and concentrated to afford the product **2** as a yellow viscous liquid (0.7 g, 67 %). ^{1}H NMR (400 MHz, $CDCl_3$, δ, ppm): 4.61 (q, *J* = 7.1 Hz, 2H, C$\underline{H}_2$CH$_3$), 4.28-4.24 (m, 2H, C$\underline{H}_2$CH$_2$OH), 3.85-3.81 (m, 2H, C$\underline{H}_2$OH), 1.64 (s, 6H, (C$\underline{H}_3$)$_2$), 1.40 (t, *J* = 7.1 Hz, 3H, CH$_2$C$\underline{H}_3$).

S-[1,2-dimethyl-4-(6-bromoisobutyrate) ethyl acetate] O-ethyl dithiocarbonate (**3**): In a two-necked 50 mL round bottom flask, **2** (500 mg, 2.0 mmol) and triethylamine (378 µL, 2.7 mmol) were dissolved in dry THF (5 mL) under inert atmosphere (N_2). The reaction mixture was cooled in an ice-water bath and a solution of α-bromoisobutyryl bromide (276 µL, 2.5 mmol) in dry THF (5 mL) was slowly added while stirring. The mixture was stirred in the ice bath for 1 h and then at room temperature for 17 h. Excess of α-bromoisobutyryl bromide was neutralised with water and the reaction mixture was poured into aqueous HCl (pH 2) and extracted with DCM. The combined organic layers were washed with saturated sodium carbonate (2 x 50 mL) and brine (2 x 50 mL), dried over $MgSO_4$ and concentrated *in vacuo*. The yellow viscous solid obtained was purified over a silica column (hexane : ethyl acetate 8:2), and the relevant fractions were combined and evaporated to afford the product **3** as a yellow viscous liquid (0.4 g, 55 %). ^{1}H NMR (400 MHz, $CDCl_3$, δ, ppm): 4.60 (q, *J* = 7.1 Hz, 2H, C$\underline{H}_2$CH$_3$), 4.42-4.35 (m, 4H, OC$\underline{H}_2$C$\underline{H}_2$O), 1.93 (s, 6H, C(C$\underline{H}_3$)$_2$), 1.62 (s, 6H, (C$\underline{H}_3$)$_2$), 1.39 (t, *J* = 7.1 Hz, 3H, C$\underline{H}_3$).

S-[1,2-dimethyl-4-(6-chloroisobutyrate) ethyl acetate] O-ethyl dithiocarbonate (**4**): The final chloroxanthate CTA **4** was prepared using a halogen exchange reaction. A 100 mL Schlenk flask was charged with **3** (2.21 g, 13.7 mmol), 2,2'-bipyridine (5.16 g, 82.4 mmol), and dry acetone (20 mL), and deoxygenated using three freeze-pump-thaw cycles. CuCl (236 mg, 2.39 mmol) and $CuCl_2$ (146 mg, 1.09 mmol) were quickly added to the frozen mixture, and the oxygen removed by a further three freeze-pump-thaw cycles. After stirring for 24 h at 50 °C, the acetone was removed and the mixture was diluted with DCM (15 mL) before passing it over a column of neutral alumina. The solution was diluted with DCM (35 mL) and washed with EDTA (100 mM, 3 x 50 mL), saturated sodium bicarbonate (1 x 50 mL) and brine (2 x 50 mL). The organic fraction was dried over $MgSO_4$, and the concentrated mixture was purified over a silica column (hexane : ethyl acetate 3:1). After combination and concentration of the relevant fractions, the product **4** was obtained as a yellow oil (0.2 g, 52 %). MS (MALDI-TOF, CHCA matrix) m/z calcd. for $C_{13}H_{21}ClO_5S_2Na$ $[M+Na]^+$ 379.1, Found. 379.1; ^{1}H-NMR (400 MHz, $CDCl_3$, δ, ppm): 4.60 (q, *J* = 7.1 Hz, 2H, C$\underline{H}_2$CH$_3$), 4.41-4.36 (m, 4H, OC$\underline{H}_2$C$\underline{H}_2$O), 1.77 (s, 6H, C(C$\underline{H}_3$)$_2$), 1.62 (s, 6H, (C$\underline{H}_3$)$_2$), 1.39 (t, *J* = 7.0 Hz, 3H, C$\underline{H}_3$); ^{13}C-NMR (100 MHz, $CDCl_3$, δ, ppm): 211.0 (C=S), 173.0 (C=O, ATRP side), 171.5 (C=O, RAFT side), 70.0 (C(CH$_3$)$_2$Cl), 64.5 (C(CH$_3$)$_2$S), 63.5 (CH$_2$OC(O)C(CH$_3$)$_2$Cl), 63.2 (CH$_2$CH$_2$OC(O)C(CH$_3$)$_2$Cl), 54.2 (CH$_3$CH$_2$), 30.0 (C(CH$_3$)$_2$Cl), 26.0 (C(CH$_3$)$_2$S), 13.5 (CH$_3$CH$_2$).

RAFT of NVP

In a typical experiment, the chloroxanthate CTA (40 mg, 0.1 mmol), AIBN (1.84 mg, 0.01 mmol) and NVP (1.87 g, 16.8 mmol) were charged to a 10 mL round bottom flask equipped with a magnetic stirrer bar and a septum with 3.4 mL of 1,4-dioxane. 1,3,5-Trioxane (90 mg, 1 mmol) was also added to the reaction mixture as a reference for calculating monomer conversion. The reaction mixture was degassed by bubbling N_2, and then transferred to a pre-heated oil bath at 65 °C for 17 h. The reaction was stopped by introducing oxygen, and 1,4-dioxane was removed under vacuum. The viscous liquid was solubilised in DCM and the polymer was purified by precipitation in hexane. Monomer conversion was determined by ^{1}H NMR using 1,3,5-trioxane as internal standard.

ARGET-ATRP of TEGMA

In a typical experiment, PVP macroinitiator (162 mg, 1.8 µmol) was mixed with TEGMA (100 mg, 430 µmol, 40 eq.), $CuCl_2$ (1.4 mg, 1.8 µmol) and the ligand TPMA (3.1 mg, 1.8 µmol) in IPA/water (50 % v/v) such that the monomer concentration in the final mixture was 0.5 M. Separately, a solution of ascorbic acid (28 mg/mL) in IPA/water (50 % v/v) was prepared, and both solutions were degassed by argon bubbling. Ascorbic acid solution (0.75 eq. relative to the initiator) was added to start the polymerisation, which was conducted at 40 °C.

Cross-linking of self-assembled block copolymers

PVP-*co*-pTEGMA (0.4 mg) was dissolved in 800 µL of 20 mM sodium acetate buffer (20 mM, pH 4) in a glass vial equipped with a septum and a magnetic stirrer. Cross-linker potassium persulphate (1.8 mM) was added to the polymer solution, followed by degassing by bubbling N_2. The reaction mixture was transferred to a pre-heated oil bath at 80 °C for 2 h and then cooled down to room temperature to confirm the structural integrity of the cross-linked structures. Prior to Transmission Electron Microscopy (TEM) imaging, the cross-linked assemblies were subjected to dialysis against water, using a Slide-A-Lyzer MINI Dialysis Device, 2 kDa MWCO (Thermo Scientific).

Characterisation techniques

NMR spectra were recorded on Bruker DPX-400 400 MHz instruments using deuterated solvents obtained from Sigma-Aldrich. Conversion for polymerisations of NVP and TEGMA were determined by ^{1}H NMR. Molecular weight distributions of the resulting polymers were characterised using size exclusion chromatography (SEC) over two PSS GRAM columns in series using DMF (+ 0.075 % w/v LiBr) as the eluent. Retention times were normalised using water as a flow rate marker and molecular weights were calculated without correction relative to a set of narrow polystyrene standards. Matrix-assisted laser desorption/ionization (MALDI) time of flight (ToF) spectra were collected on a Waters Micromass MALDI-ToF in positive ion reflectron mode, calibrated using poly(ethylene glycol) standards. TEM images of the polymer nanostructures were recorded on a JEOL JEM 2100 field emission electron microscope, operating with an acceleration voltage of 200 kV. The TEM samples were prepared by dropping 5 µL of a solution of the cross-linked self-assembled copolymers onto mesh copper grids and subsequently dried at room temperature. The grids were stained with a solution of 0.2 % w/w uranyl acetate. Size distribution measurements were performed using a Zetasizer Nano ZS (Malvern). In all dynamic light scattering (DLS) measurements, the scattering angle was fixed at 173°. DLS was also used to measure the temperature-responsive behaviour of PVP-*co*-pTEGMA. Solutions of PVP-*co*-pTEGMA (2 mg/mL in 20 mM NaOAc pH 4) were submitted to a temperature ramp (1 °C) with 30 s equilibration time. Each data point corresponds to the average of 5 measurements of 10 s with an attenuator value fixed at 8 and a measurement position set up at 4.65 mm.

Results and Discussion

Polymer synthesis

Given the vastly divergent activities of NVP and TEGMA, the synthesis of PVP-*co*-pTEGMA copolymers could not be done using traditional means. We chose to prepare these polymers through a control agent able to act as both a chain transfer agent in RAFT polymerisation and as an initiator for ATRP reactions. We chose to use RAFT to control NVP polymerisation following promising findings in literature studies.[13,14] Since NVP is the less active monomer, we performed this reaction before chain extension of the polymer from the ATRP initiator with TEGMA. The CTA (Figure 1, compound **4**) was therefore designed to have a Z group suitable for NVP, following previous work by Matyjaszewski and coworkers.[31] Unlike in their study, we included two methyl substituents rather than one substituent on the R group of the RAFT agent in an attempt to reduce the inhibition period at the start of the RAFT polymerisation. Since bromoxanthate CTAs have been shown to lead to almost quantitative dimerisation of NVP in RAFT polymerisations,[25] a chloroxanthate CTA was used for initiation of the ATRP reaction. No such dimerisations have been observed with chloroxanthate agents.[25] Additionally, xanthate CTA has been shown to have a very low efficiency as a radical transfer agent for methyl methacrylates,[25] ensuring the regioselectivity of the ARGET-ATRP of TEGMA without interference of the RAFT moiety in the CTA.

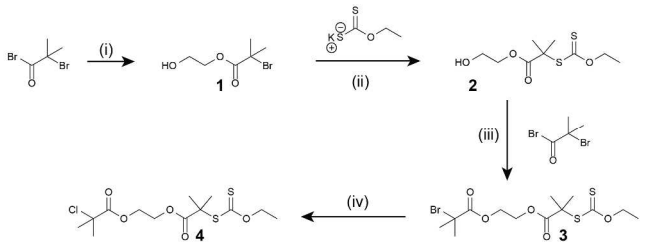

Fig. 1 Synthesis of chloroxanthate chain transfer agent (CTA) (compound **4**). (i) Ethylene glycol/pyridine/THF, (ii) acetone, (iii) triethylamine/THF. (iv) CuCl/$CuCl_2$/2,2'-bipyridine/acetone.

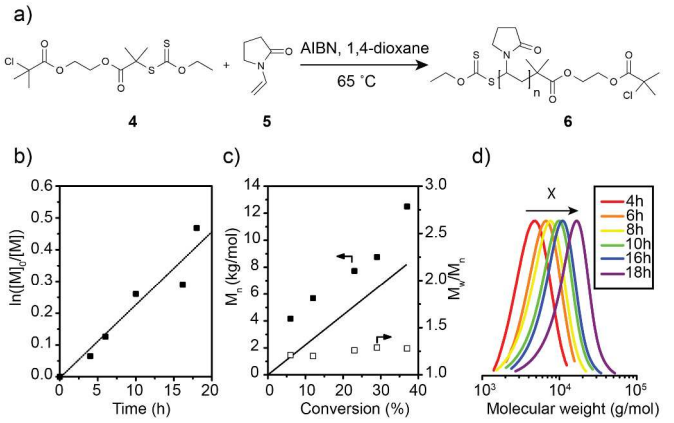

Fig. 2 Synthesis of PVP by RAFT (compound **6**). a) Synthetic scheme. b) Kinetic plot of monomer conversion *versus* time. c) Plots showing the evolution of M_n (filled squares) and dispersity (open squares) *versus* conversion. d) Evolution of GPC traces during NVP polymerisation. ([CTA] / [I] / [NVP] = 1 / 0.1 / 200; [NVP] = 5 M)

A schematic of RAFT polymerisation of NVP, using a M:CTA:I ratio of 200:1:0.1 is shown in Figure 2a. Robust control was observed even at a high monomer concentration of 5 M as seen by the pseudo-first order kinetics (Figure 2b), a linear increase of molecular weight *versus* monomer conversion, and narrow molecular weight distribution (M_w/M_n < 1.3, Figure 2c-d). No significant inhibition period was observed as had been reported in previous work with a similar RAFT agent,[31] presumably due to the additional methyl substituent on the R group. Table 1 summarises the properties of PVP homopolymers.

Table 1 Library of PVP polymers synthesised

#	[NVP]:[CTA]	Time (h)	X (%)	M_n (Da) (NMR)	M_n (Da) (GPC)	M_w/M_n
6a	160	17	27	4800	6220	1.22
6b	300	17	27	9000	17130	1.25
6c	400	17	31	13780	16490	1.26
6d	500	17	27	15000	18220	1.27
6e	750	17	22	18340	22530	1.34

Table 2 Library of PVP-*co*-pTEGMA block copolymers synthesised

#	PVP M_w (kDa)	[TEGMA] / [CTA]	Time (h)	X (%)	M_n (Da) (NMR)	M_n (Da) (GPC)	M_w/M_n	wt % TEGMA	T_{cp} (°C)	Z-average (nm) (PDI)	
										Pre-XL @ 65 °C	Post-XL @ 25 °C
8a	9.0	40	5	47	5030	14420	1.38	33%	61	217 (0.17)	274 (0.10)
8b	9.0	75	17	37	6270	16630	1.54	42%	54	212 (0.13)	136 (0.07)
8c	15.0	40	5.4	57	4180	17660	1.41	26%	60	221 (0.18)	225 (0.10)
8d	15.0	75	17	47	11610	18590	1.62	35%	57	185 (0.10)	110 (0.09)
8e	15.0	40	17	99	-	26780	1.50	38%	58	277 (0.10)	175 (0.10)

We chose two homopolymers, PVP 9 kDa and 15 kDa (**6**b and **6**d, respectively), as macroinitiators for the subsequent block extension with TEGMA *via* ARGET-ATRP, as their polydispersities were below 1.3 and we were interested to see if the difference in molecular weight of the PVP block would lead to variation in the properties of the block copolymers. The chain extension of these PVP macroinitiators was performed using ARGET-ATRP (Figure 3a). By using ARGET-ATRP rather than standard ATRP, which has been used in the only other example of a PVP chain extension,[26] the demand for copper and intolerance to oxygen was reduced. The chain extension of the two different PVP macroinitiators (9 kDa and 15 kDa) demonstrated linear pseudo-first order kinetics (Figure 3b), and a linear evolution of molecular weight *versus* conversion (Figure 3c). The molecular weight distribution stayed in a relatively narrow range ($M_w/M_n \leq 1.5$) with only a small amount of tailing (Figure 3c-d), which demonstrated the successful synthesis of well-defined PVP-*co*-pTEGMA block copolymers. The library of copolymers synthesised is reported in Table 2.

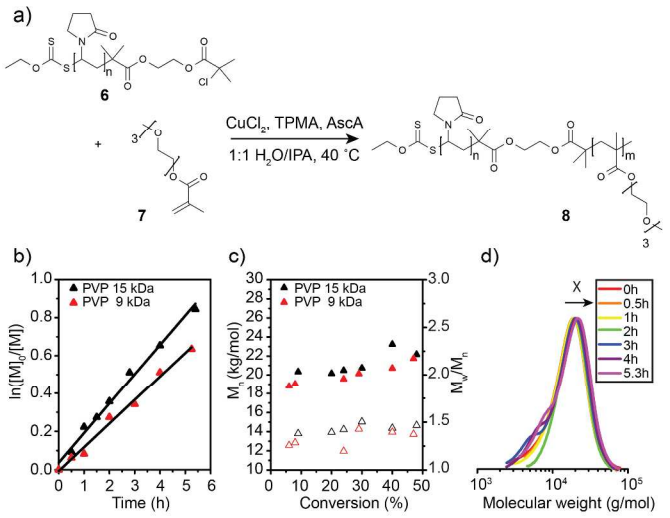

Fig. 3 Synthesis of PVP-*co*-pTEGMA block copolymers *via* chain extension of PVP macroinitiators with TEGMA by ARGET-ATRP (compound **8**). a) Synthetic scheme. b) Kinetic plots of monomer conversion *versus* time. c) Plots showing the evolution of M_n (filled symbols) and dispersity (open symbols) *versus* conversion. d) Evolution of GPC traces during TEGMA polymerisation. ([TEGMA] / [CTA] = 40 / 1; [TEGMA] = 0.5 M)

Self-assembly and cross-linking

Following the successful synthesis of PVP-*co*-pTEGMA, we investigated the temperature-responsive behaviour of these block copolymers. Both pTEGMA and PVP homopolymers are known to display temperature-responsive behaviour.[27,32] The LCST for PVP can be observed above the boiling temperature of water,[32] while the LCST for pTEGMA is around 52 °C.[27] We hypothesised that while PVP-*co*-pTEGMA copolymers should be soluble in water at room temperature, at the LCST of pTEGMA the polymer will undergo a drastic conformational and solubility change (known as the coil-globule transition) driven by the sensitive dehydration behaviour and leading to a collapse of the polymer chains caused by the increased favourability of hydrophobic interactions between polymer chains relative to polymer-water interactions.[27] To confirm this, we first determined the cloud point temperature (T_{cp}) of PVP-*co*-pTEGMA copolymers using Dynamic Light Scattering (DLS). Figure 4a shows the evolution of count-rate at 1 °C resolution as the temperature in the instrument was ramped. Each measurement was made at a fixed position and with a fixed attenuator, so the count-rate is proportional to the total intensity of scattered light, and therefore the assembly of the copolymers. T_{cp} was determined by the inflection points of the curves and we found that the T_{cp} of the copolymers varied between 54 °C and 61 °C (Figure 4a, Table 2), in accordance with the LCST for pTEGMA previously reported.[27] Studies have reported the very small influence of the DP_n of poly(oligo[ethylene glycol] methacrylates) on the value of their LCST,[28,33] which is in agreement with this study. Contrary to pTEGMA homopolymers, these copolymer solutions did not evolve into cloudy, opaque solutions when the temperature reached the T_{cp} of pTEGMA, indicating that copolymers were self-assembling instead of forming precipitates. To confirm this phenomenon, we investigated the size distribution of the copolymer assemblies (PVP-*co*-pTEGMA copolymers **8**a-**8**e in Table 2) at 65 °C, above the T_{cp}, by DLS (Figure 4b and Supporting information, Figure S1). The size of the resulting structures varied between 180 nm and 280 nm in diameter (Figure 4b, Table 2). When these structures were subjected to temperature below their T_{cp}, we observed significant changes in size distributions to below 10 nm for all of the copolymer assemblies (Figure 4b), indicating the disassembly of the structures. To obtain self-assembled structures that can retain their integrity at physiological conditions, the copolymers need to be cross-linked. PVP is a versatile polymer with ease of cross-linking by gamma rays, strong alkaline, peroxides, and inorganic persulphates.[34] We exploited this to covalently cross-link the self-assembled PVP-*co*-pTEGMA structures using potassium persulphate.[34] The mechanism of cross-linking of

PVP with potassium persulphate is believed to proceed *via* self-condensation of the PVP, following abstraction of an hydrogen atom on the polymer backbone.[34] The size of the self-assembled PVP-*co*-pTEGMA structures after cross-linking with potassium persulphate are shown in Figure 4b and Table 2, confirming the successful cross-linking and the stability of the structures below the T_{cp}. Dialysis against water did not affect the size of the aggregates (Supporting information, Figure S2), confirming the stability of the cross-linking mechanism in solutions of various ionic strengths.

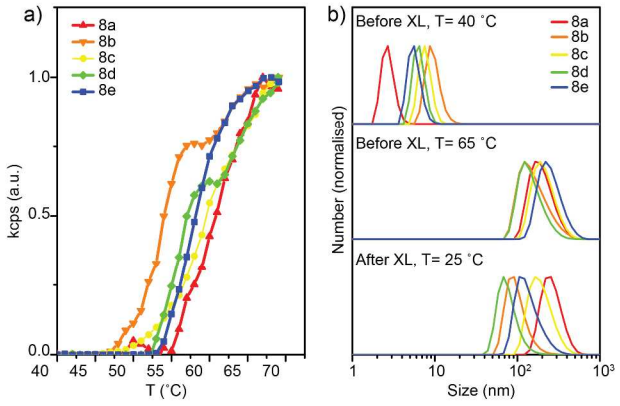

Fig. 4 Temperature-triggered self-assembly of PVP-*co*-pTEGMA block copolymers. a) Evolution of count-rate *versus* temperature measured by DLS. The cloud point temperature (T_{cp}) of each copolymer was determined by the inflection points of the curves. b) Normalised size distribution as determined by DLS of PVP-*co*-pTEGMA (2 mg/mL copolymer solution in 20 mM NaOAc pH 4) below the T_{cp} at 40 °C, and self-assembled PVP-*co*-pTEGMA before and after cross-linking (XL) with potassium persulphate, at 65 °C and 25 °C, respectively, confirming the structural integrity of the cross-linked structures below the T_{cp}.

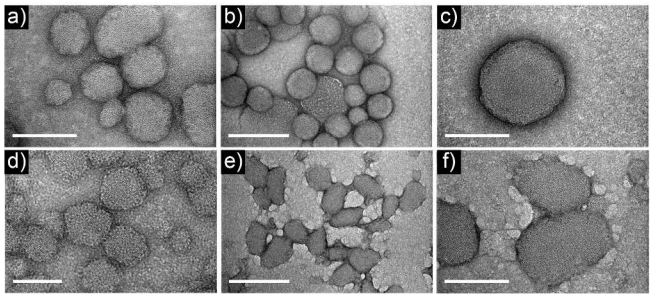

Fig. 5 TEM images illustrating the structures of self-assembled PVP-*co*-pTEGMA *post* cross-linking with potassium persulphate. a) **8**b (scale bar 200 nm), b) **8**c (scale bar 500 nm), c) **8**c at higher magnification (scale bar 100 nm), d) **8**d (scale bar 100 nm), e) **8**e (scale bar 500 nm), f) **8**e at higher magnification (scale bar 200 nm).

To further confirm the morphology of the self-assembled PVP-*co*-pTEGMA structures, we used Transmission Electron Microscopy (TEM) to image the dialysed cross-linked PVP-*co*-pTEGMA polymers. Relatively monodisperse spherical aggregates were observed, with sizes that corresponded well to the DLS measurements (Figure 4b, Table 2) and which are consistent with other polymersomes in the literature.[35] This temperature triggered self-assembly of PVP-*co*-pTEGMA into precise architectures at the nanoscale is particularly interesting for applications in drug delivery and the design of smart, stimuli-responsive materials.

Conclusions

We demonstrated successful synthesis of well-defined PVP-*co*-pTEGMA block copolymers by successive RAFT and ARGET-ATRP. We showed that PVP-*co*-pTEGMA block copolymers self-assembled above their cloud point temperature (T_{cp}) into large spherical nanostructures, and that these assemblies could be stabilised below their T_{cp} by cross-linking them through the PVP block. These new materials present new and exciting opportunities for the development of novel biomaterials and drug delivery carriers.

Acknowledgements

C.J. and M.M.S gratefully acknowledge financial support from the Rosetrees trust. R.C. acknowledges the support of Marie Curie International Incoming Fellowship within the 7th European Community Framework Programme. M.M.S received funding from an ERC Consolidator grant "Naturale CG".

Notes and references

Department of Materials, Department of Bioengineering, and Institute of Biomedical Engineering, Imperial College London, London, SW7 2AZ, United Kingdom.
E-mail: m.stevens@imperial.ac.uk

Electronic Supplementary Information (ESI) available: Size distribution by intensity of PVP-*co*-pTEGMA before and after cross-linking and before and after dialysis, and MALDI-TOF of the chloroxanthate CTA. See DOI: 10.1039/b000000x

1. S. Lowe, N. M. O'Brien-Simpson, L. A. Connal. *Polym. Chem.*, 2015, **6**, 198–212.
2. A. N. Zelikin, G. K. Such, A. Postma, F. Caruso. *Biomacromolecules*, 2007, **8**, 2950–2953.
3. W. Sun, Z. Araci, M. Inayathullah, S. Manickam, X. Zhang, M. A. Bruce, M. P. Marinkovich, A. T. Lane, C. Milla, J. Rajadas, M. J. Butte. *Acta Biomater.*, 2013, **9**, 7767–7774.
4. R. Chandrawati, S.-F. Chong, A. N. Zelikin, L. Hosta-Rigau, B. Städler, F. Caruso. *Soft Matter*, 2011, **7**, 9638–9646.
5. N. Ruecha, R. Rangkupan, N. Rodthongkum, O. Chailapakul. *Biosens. Bioelectron.*, 2014, **52**, 13–19.
6. L. Rodríguez-Lorenzo, R. de la Rica, R. A. Álvarez-Puebla, L. M. Liz-Marzán, M. M. Stevens. *Nat. Mater.*, 2012, **11**, 604–607.
7. C. E. Hoppe, M. Lazzari, I. Pardiñas-Blanco, M. A. López-Quintela. *Langmuir*, 2006, **22**, 7027–7034.
8. H. Wang, X. Qiao, J. Chen, X. Wang, S. Ding. *Mater. Chem. Phys.*, 2005, **94**, 449–453.
9. G. Moad, E. Rizzardo, S. H. Thang. *Aust. J. Chem.*, 2005, **58**, 379–410.
10. K. Matyjaszewski. *Macromolecules*, 2012, **45**, 4015–4039.
11. K. Nakabayashi, H. Mori. *Eur. Polym. J.*, 2013, **49**, 2808–2838.
12. X. Lu, S. Gong, L. Meng, C. Li, S. Yang, L. Zhang. *Polymer*, 2007, **48**, 2835–2842.
13. R. Devasia, R. L. Bindu, R. Borsali, N. Mougin, Y. Gnanou. *Macromol. Symp.*, 2005, **229**, 8–17.

14. D. Wan, K. Satoh, M. Kamigaito, Y. Okamoto. *Macromolecules*, 2005, **38**, 10397–10405.
15. A. Postma, T. P. Davis, G. Li, G. Moad, M. S. O'Shea. *Macromolecules*, 2006, **39**, 5307–5318.
16. J. Chiefari, R. T. Mayadunne, C. L. Moad, G. Moad, E. Rizzardo, A. Postma, M. A. Skidmore, S. H. Thang. *Macromolecules*, 2003, **36**, 2273–2283.
17. G. Moad, E. Rizzardo, S. H. Thang. *Aust. J. Chem.*, 2006, **59**, 669–692.
18. D. J. Keddie. *Chem. Soc. Rev.*, 2013, **43**, 496–505.
19. D. Quémener, T. P. Davis, C. Barner-Kowollik, M. H. Stenzel. *Chem. Commun.*, 2006, 5051–5053.
20. M. Benaglia, J. Chiefari, Y. K. Chong, G. Moad, E. Rizzardo, S. H. Thang. *J. Am. Chem. Soc.*, 2009, **131**, 6914–6915.
21. D. J. Keddie, C. Guerrero-Sanchez, G. Moad, E. Rizzardo, S. H. Thang. *Macromolecules*, 2011, **44**, 6738–6745.
22. K. V. Bernaerts, F. E. Du Prez. *Prog. Polym. Sci.*, 2006, **31**, 671–722.
23. H. U. Kang, Y. C. Yu, S. J. Shin, J. Kim, J. H. Youk. *Macromolecules*, 2013, **46**, 1291–1295.
24. A. Veeren, A. Bhaw-Luximon, D. Jhurry. *Eur. Polym. J.*, 2013, **49**, 3034–3045.
25. C. F. Huang, R. Nicolay, Y. Kwak, F. C. Chang, K. Matyjaszewski. *Macromolecules*, 2009, **42**, 8198–8210.
26. C. F. Huang, R. Nicolay, Y. Kwak, F. C. Chang, K. Matyjaszewski. *Macromolecules*, 2009, **42**, 8198–8210.
27. J. F. Lutz. *J. Polym. Sci. Part A Polym. Chem.*, 2008, **46**, 3459–3470.
28. J.-F. Lutz, O. Akdemir, A. Hoth. *J. Am. Chem. Soc.*, 2006, **128**, 13046–13047.
29. M. Yamato, Y. Akiyama, J. Kobayashi, J. Yang, A. Kikuchi, T. Okano. *Prog. Polym. Sci.*, 2007, **32**, 1123–1133.
30. K. Min, H. Gao, K. Matyjaszewski. *J. Am. Chem. Soc.*, 2005, **127**, 3825–3830.
31. R. Nicolaÿ, Y. Kwak, K. Matyjaszewski. *Chem. Commun.*, 2008, 5336–5338.
32. P. Sakellariou. *Polymer*, 1992, **33**, 1339–1342.
33. C. Weber, R. Hoogenboom, U. S. Schubert. *Prog. Polym. Sci.*, 2012, **37**, 686–714.
34. C. C. Anderson, F. Rodriguez, D. A. Thurston. *J. Appl. Polym. Sci.*, 1979, **23**, 2453–2462.
35. R. P. Brinkhuis, F. P. J. T. Rutjes, J. C. M. van Hest. *Polym. Chem.*, 2011, **2**, 1449.